

## Supplementary Information for:

### The effect of rigidity on the emission of quadrupolar strongly polarized dyes

Bartosz Szymański,<sup>a,d</sup> Smruti Ranjan Sahoo,<sup>b</sup> Rashid Valiev,<sup>c</sup> Olena Vakuliuk,<sup>a</sup> Piotr Łaski,<sup>d</sup> Katarzyna N. Jarzemska,<sup>d</sup>  
Radosław Kamiński,<sup>\*d</sup> Glib Baryshnikov,<sup>\*b</sup> Mohammad B. Teimouri,<sup>\*a,e</sup> and Daniel T. Gryko<sup>\*a</sup>

<sup>a</sup>Institute of Organic Chemistry, Polish Academy of Sciences, Kasprzaka 44/52, 01-224 Warsaw, Poland

<sup>b</sup>Laboratory of Organic Electronics, Department of Science and Technology, Linköping University, SE-60174 Norrköping, Sweden

<sup>c</sup>Department of Chemistry, University of Helsinki, FI-00014 Helsinki, Finland

<sup>d</sup>Department of Chemistry, University of Warsaw, Żwirki i Wigury 101, 02-089 Warsaw, Poland

<sup>e</sup>Faculty of Chemistry, Kharazmi University, 15719-14911 Tehran, Iran

## Table of Contents

1. General remarks .....	2
2. Synthetic procedures.....	3
3. <sup>1</sup> H and <sup>13</sup> C NMR spectra for synthesized compounds.....	6
4. Optical properties (in solution) .....	10
5. Optical properties (in solid state) .....	12
6. Crystallographic data.....	14
7. Theoretical calculations.....	17
8. References .....	32

# 1. General remarks

All chemicals were used as received unless otherwise noted. Transformations with moisture and oxygen sensitive compounds were performed under a stream of argon. The reaction progress was monitored by means of thin layer chromatography (TLC), which was performed on aluminium foil plates, covered with Silica gel 60 F254 (Merck). The identity and purity of prepared compounds were proved by  $^1\text{H}$  NMR and  $^{13}\text{C}$  NMR spectroscopy as well as by MS-spectrometry (via APCI-MS or EI-MS). NMR spectra were measured on Varian 500 MHz and Varian 600 MHz instruments. Chemical shifts for  $^1\text{H}$  NMR are expressed in parts per million (ppm) relative to tetramethylsilane ( $\delta$  0.00 ppm),  $\text{CDCl}_3$  ( $\delta$  7.26 ppm) or  $[\text{D}_2]\text{-TCE}$  ( $\delta$  5.91 ppm). Chemical shifts for  $^{13}\text{C}$  NMR are expressed in ppm relative to  $\text{CDCl}_3$  ( $\delta$  77.0 ppm) or  $[\text{D}_2]\text{-TCE}$  ( $\delta$  72.4 ppm). Data are reported as follows: chemical shift, multiplicity (s = singlet, d = doublet, dd = doublet of doublets, t = triplet, td = triplet of doublets, q = quartet, quint = quintet, sex = sextet, m = multiplet), coupling constant (in Hz), and integration. All melting points for crystalline products were measured with automated melting point apparatus EZ-MELT and were given without correction.

Spectrophotometric grade solvents were used without further purification. All photophysical studies were performed with freshly-prepared, air equilibrated solutions at room temperature. Steady-state fluorescence measurements were performed in standard 1 cm quartz cuvettes with dilute solutions ( $10^{-6}$  M, optical density  $<0.1$ ) to minimize inner filter effects and/or aggregation.

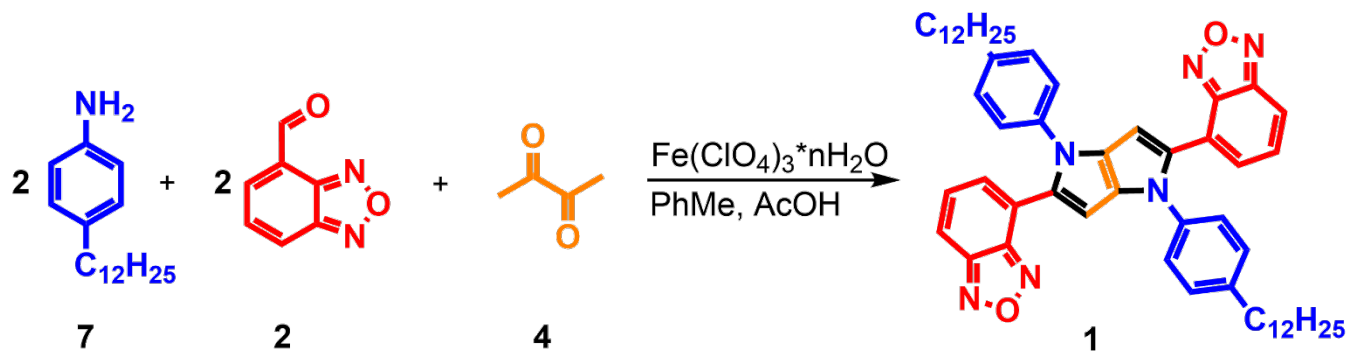
Absorption spectra were measured using UV-Vis Shimadzu UV-3600i Plus spectrophotometer. The calculation of molar absorption coefficient were conducted from Lambert-Beer's law equation.

Emission spectra were measured using Edinburgh Instruments FS5 spectrofluorometer equipped with photomultiplier Hamamatsu R123456. Fluorescence quantum yields ( $\Phi$ ) were calculated from equation:

$$\Phi = \Phi_{st} \cdot \frac{(1 - 10^{-A_{st}}) \cdot n^2 \cdot S}{(1 - 10^{-A}) \cdot n_{st}^2 \cdot S_{st}}$$

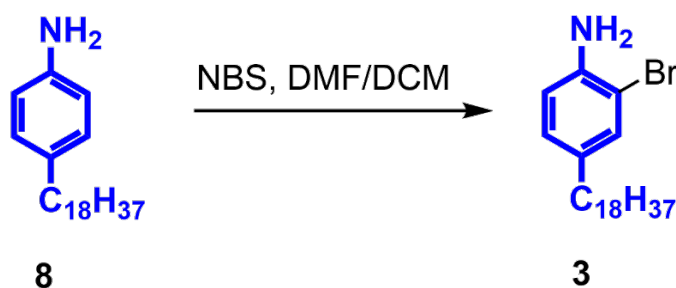
Where  $A$  denotes absorbance,  $n$  is a refractive index of a solvent and  $S$  is an integrated fluorescence intensity.

## 2. Synthetic procedures



Scheme S1. Synthesis of centrosymmetric TAPP **1**.

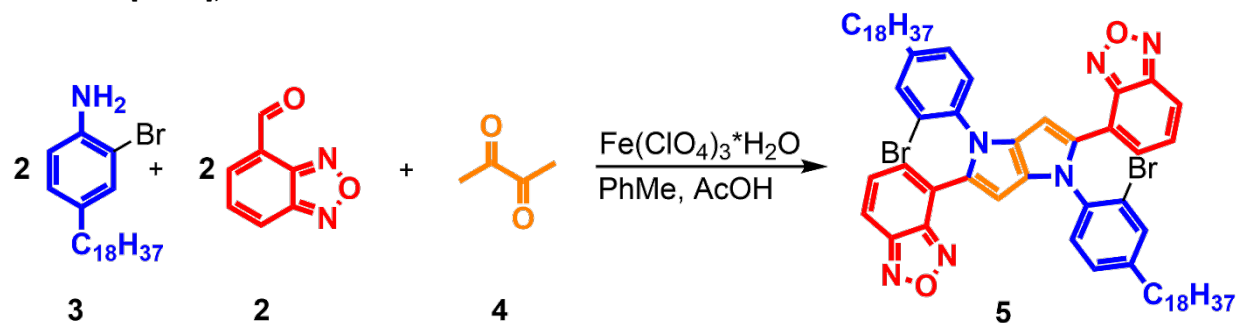
**2,5-bis(4-(2,1,3-benzoxadiazolyl))-1,4-bis(4-dodecylphenyl)-1,4-dihydropyrrolo[3,2-*b*]pyrrole (**1**):** Glacial acetic acid (2 mL), toluene (2 mL), benzo[*c*][1,2,5]oxadiazole-4-carbaldehyde (**2**, 296.2 mg, 2 mmol, 2 eq.) and 4-dodecylaniline (**7**, 522.8 mg, 2 mmol, 2 eq.) were placed in a 50 mL round-bottom flask equipped with a magnetic stir bar. The mixture was reacted at 50°C for 1 h. After that time, Fe(ClO<sub>4</sub>)<sub>3</sub>·xH<sub>2</sub>O (20 mg, 5 mol%) was added, followed by butane-2,3-dione (**4**, 87 μL, 1 mmol, 1 eq.). The resulting mixture was stirred at 50 °C (oil bath) in an open flask under air overnight. Next, 3 mL of acetonitrile was added and the flask with reaction mixture was moved to the fridge. Upon an hour crude **1** was filtered off, washed with acetonitrile and recrystallized from dichloromethane/acetonitrile mixture affording 406.6 mg (49%) of pure product as dark red solid. M.p. 91-92 °C (DCM/ACN). <sup>1</sup>H NMR (500 MHz, Chloroform-*d*) δ = 7.64 (dd, *J* = 9.4, 1.0 Hz, 2H, BOD), 7.48-7.47 (m, 2H, BOD), 7.39 (dd, *J* = 9.4, 1.5 Hz, 2H, BOD), 7.25 (s, 8H, Ar), 6.59 (s, 2H, TAPP), 2.69 – 2.63 (m, 4H, Alk), 1.68 – 1.64 (m, 4H, Alk), 1.37 – 1.33 (m, 8H, Alk), 1.33 – 1.25 (m, 28H, Alk), 0.88 (t, *J* = 6.8 Hz, 6H, Alk) ppm. <sup>13</sup>C{<sup>1</sup>H}NMR (126 MHz, Chloroform-*d*) δ = 149.7, 148.4, 141.8, 137.3, 134.9, 131.5, 131.2, 129.6, 126.9, 125.5, 122.0, 112.4, 99.3, 35.5, 31.9, 31.3, 29.7 (2 signals), 29.6 (2 signals), 29.5, 29.3 (2 signals), 22.7, 14.1 ppm. HRMS (APCI): *m/z* calculated for C<sub>54</sub>H<sub>67</sub>N<sub>6</sub>O<sub>2</sub>: 831.5326 [M+H<sup>+</sup>]; found: 831.5331.



Scheme S2. Synthesis of 2-bromo-4-octadecylaniline (**3**).

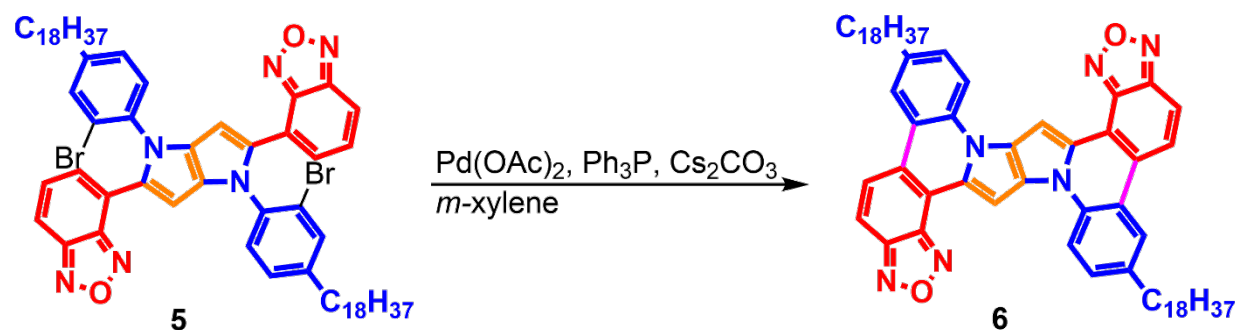
**2-bromo-4-octadecylaniline (3):** A solution of NBS (2.0 g, 12 mmol, 1 eq.) in DMF (20 mL) was added dropwise to the cooled in ice-bath solution of 4-octadecylaniline (**8**, 4.4 g, 12 mmol, 1eq.) in CH<sub>2</sub>Cl<sub>2</sub> (35 mL). The resulted mixture was stirred overnight at room temperature. Subsequently, reaction was quenched with 100 mL of water and extracted with CHCl<sub>3</sub> (3 × 50 mL). Next, combined organic layers were washed with brine, dried over MgSO<sub>4</sub>, and concentrated. The residue was crystallized from DCM to afford 4.2 g (82%) of the desired product. M.p.: 62-63 °C (DCM). <sup>1</sup>H NMR (600 MHz, Chloroform-*d*) δ 7.22 (d, *J* = 2.0 Hz, 1H, Ar), 6.91 (dd, *J* = 8.1, 2.0 Hz, 1H, Ar), 6.69 (d, *J* = 8.1 Hz, 1H, Ar), 3.93 (bs, 2H, NH<sub>2</sub>), 2.49 – 2.43 (m, 2H, Alk), 1.57 – 1.50 (m, 2H, Alk), 1.33 – 1.21 (m, 30H, Alk), 0.88 (t, *J* = 7.0 Hz, 3H, Alk) ppm. <sup>13</sup>C{<sup>1</sup>H} NMR (151 MHz, Chloroform-*d*) δ 141.4, 134.7, 132.1, 128.4, 115.9, 109.5, 34.7,

31.9, 31.6, 29.7 (2 peaks), 29.6, 29.5 (2 peaks), 29.4, 29.3, 22.7, 14.1. HRMS (APCI):  $m/z$  calculated for  $C_{24}H_{43}NBr$ : 424.2590  $[M+H^+]$ ; found: 424.2579.



Scheme S3. Synthesis of centrosymmetric TAPP 5.

**2,5-bis(4-(2,1,3-benzoxadiazolyl))-1,4-bis(2-bromo-4-octadecylphenyl)-1,4-dihydropyrrolo[3,2-*b*]pyrrole (5):** Glacial acetic acid (0.5 mL), toluene (1.0 mL), benzo[*c*][1,2,5]oxadiazole-4-carbaldehyde (**2**, 296.2 mg, 2 mmol, 2 eq.) and 2-bromo-4-octadecylaniline (**3**, 849.0 mg, 2 mmol, 2 eq.) were placed in a 50 mL round-bottom flask equipped with a magnetic stir bar. The mixture was stirred at 50 °C for 1 h. After that time,  $Fe(ClO_4)_3 \cdot xH_2O$  (20 mg, 5 mol%) was added, followed by butane-2,3-dione (**4**, 87  $\mu$ L, 1 mmol, 1 eq.). The resulting mixture was stirred at 50 °C (oil bath) in an open flask under air for 8h and then concentrated. The solid residue was washed with acetonitrile (2x 15 mL) and recrystallized from DCM/ $Et_2O$ /Hexanes to afford 542.6 mg (47%) of **5** as a mixture of atropoisomers. M.p.: 113-114 °C (DCM/ $Et_2O$ /Hexanes).  $^1H$  NMR (500 MHz, Chloroform-*d*)  $\delta$  = 7.63-7.61 and 7.57 - 7.54 (2 x m, 2H, BOD), 7.50 and 7.49 (2 x d,  $J$  = 8.9 Hz, 2H, BOD), 7.41 (d,  $J$  = 8.0 Hz, 1H, BOD), 7.23 (dd,  $J$  = 8.1, 2.0 Hz, 1H, BOD), 7.19 – 7.06 (m, 6H, Ar), 6.59 (m, 2H, TAPP), 2.74 – 2.61 (m, 4H), 1.76 - 1.62 (m, 4H), 1.46 – 1.16 (m, 60H), 0.88 (t,  $J$  = 6.8 Hz, 6H) ppm.  $^{13}C\{^1H\}$  NMR (126 MHz, Chloroform-*d*)  $\delta$  = 149.7, 148.2 (2 signals), 145.2, 145.1, 136.6, 136.5, 135.1, 134.7, 133.8, 132.5, 132.5, 131.6, 129.7, 128.9, 128.8, 125.4, 124.9, 122.2, 121.9, 112.4, 100.1, 99.4, 35.3, 31.9, 31.1, 29.6 (3 signals), 29.4, 29.3 (2 signals), 22.6, 14.1 ppm. S: HRMS (APCI):  $m/z$  calculated for  $C_{66}H_{89}N_6O_2Br_2$ : 1155.5414  $[M+H^+]$ ; found: 1155.5399.

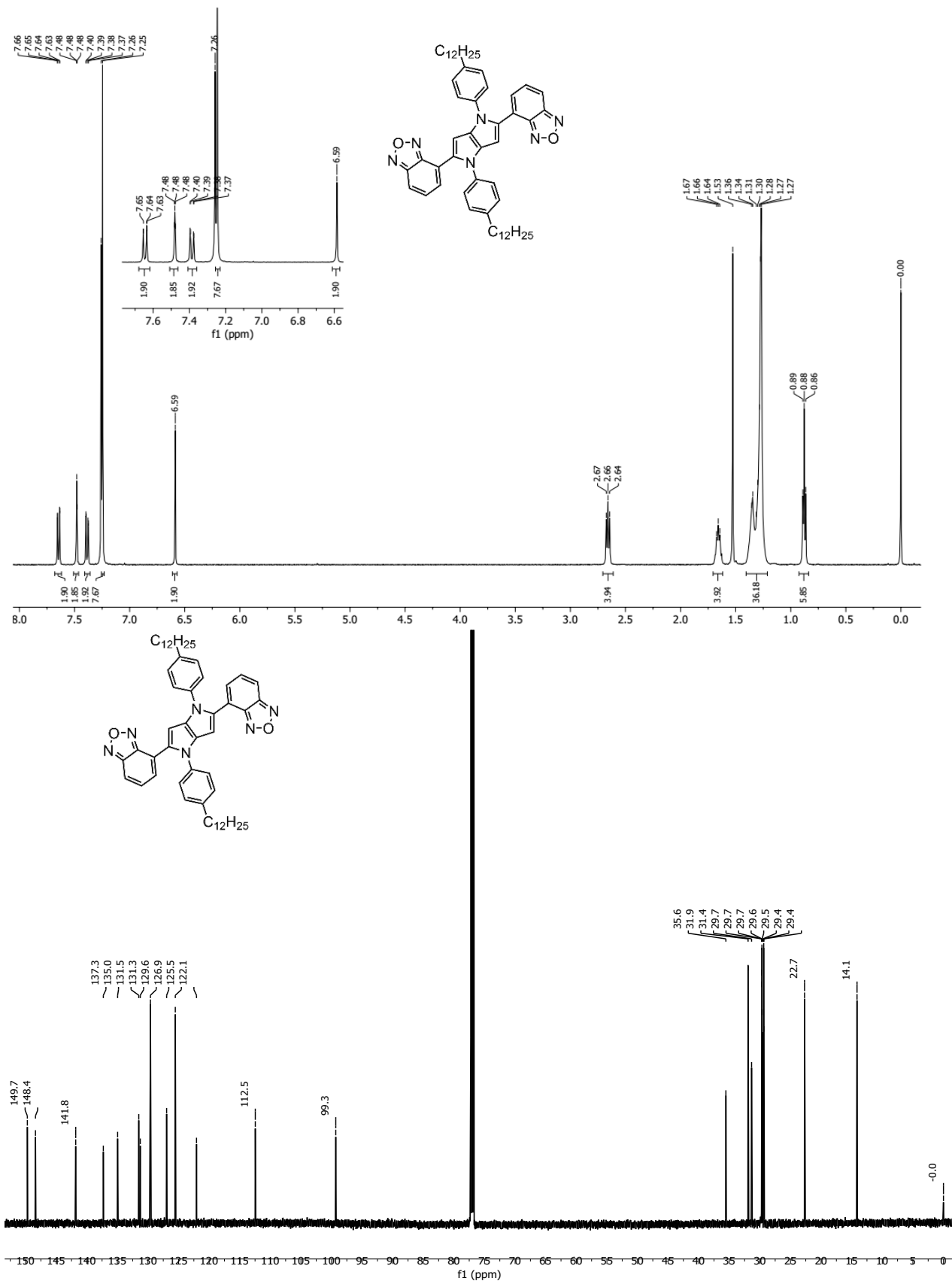


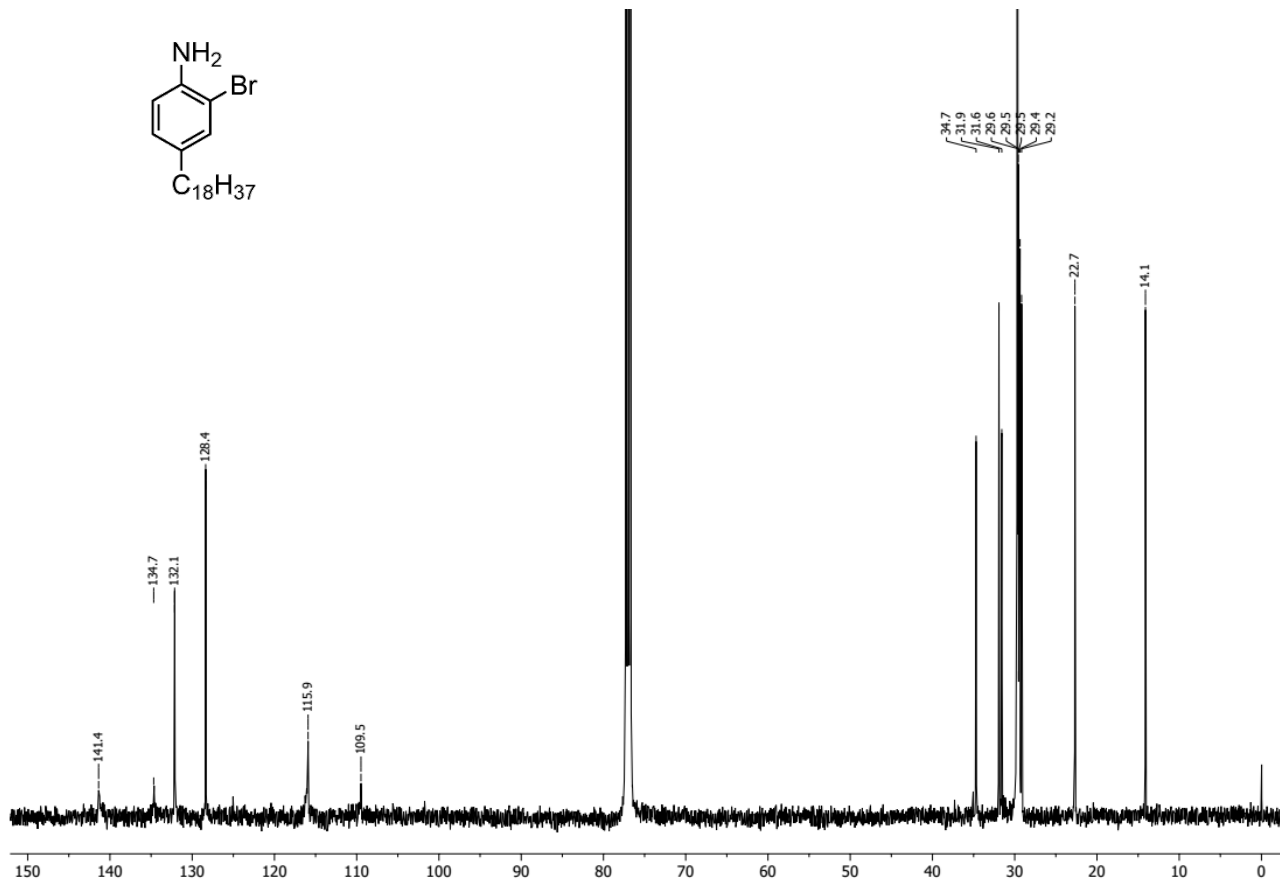
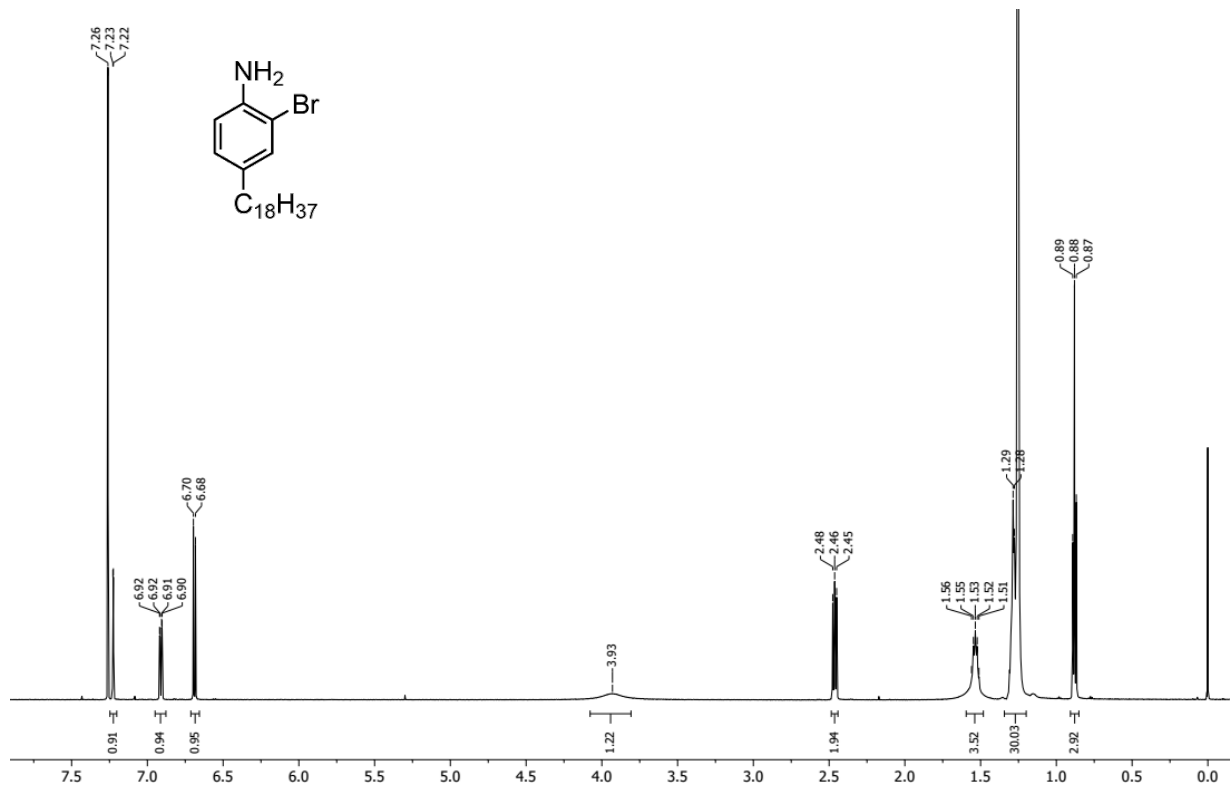
Scheme S4. Synthesis of fused TAPP 6.

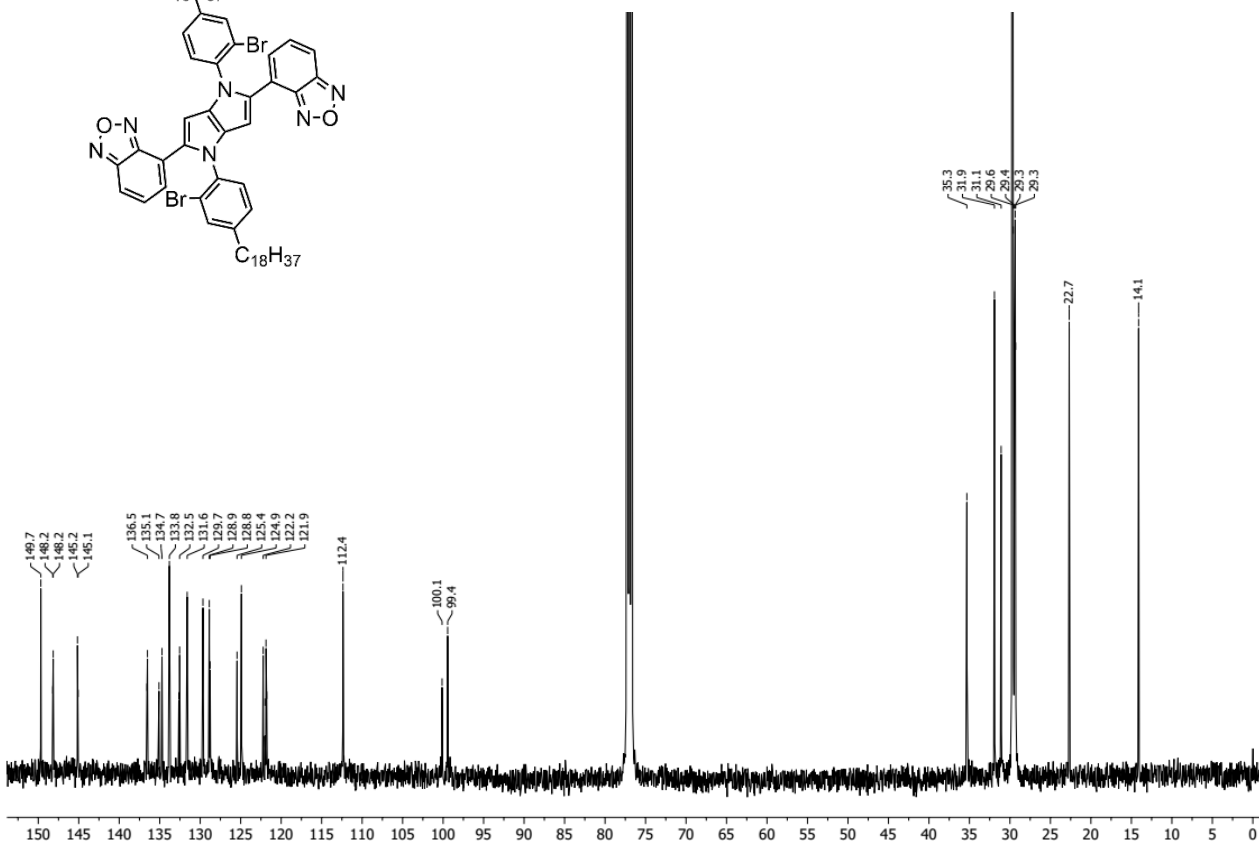
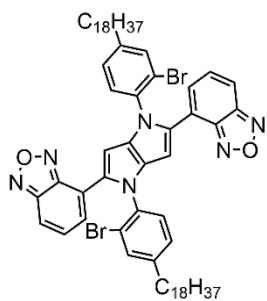
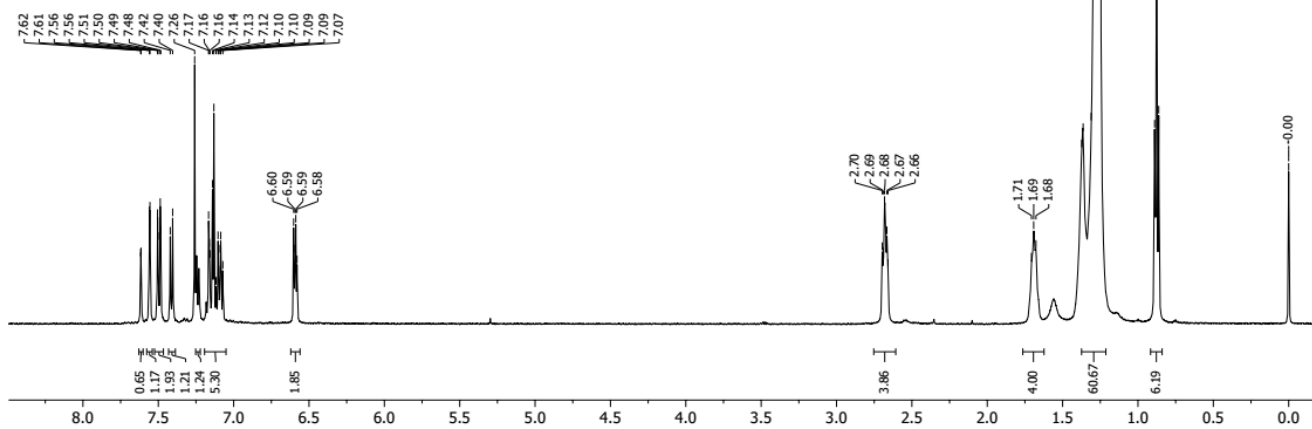
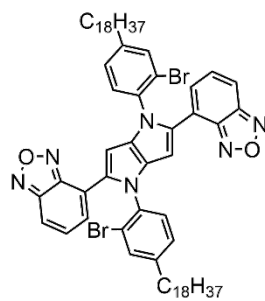
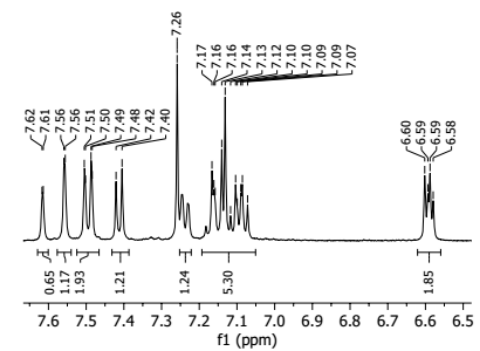
**Fused dye (6):** The Schenk flask was charged with di-brominated TAPP **5** (92.4 mg, 0.08 mmol, 1 eq.),  $Ph_3P$  (20.9 mg, 0.08 mmol, 1 eq.),  $Cs_2CO_3$  (117.0 mg, 0.36 mmol, 4.5 eq.) and  $Pd(OAc)_2$  (7.2 mg, 40 mol%). Then, dry *m*-xylene (6 ml) was added, resulting mixture was degassed 3 times and stirred at 150 °C overnight. After cooling to around 80°C, toluene (10 mL) was added and resulting suspension was filtered. The resulted precipitate was washed with water (50ml) and cold toluene (10ml) to afford 73.3 mg (92%) of **6** as green-grey solid. To obtain sample for optical measurements, 50 mg of **6** were dissolved in boiling toluene and passed through a pad of Celite (washed with boiling toluene), all filtrates were concentrated to ca. 5 ml and 9.9 mg of **6** as green-grey solid was filtered off (the loss caused by the limited solubility of **6**). M.p.: 236-238 °C (toluene).  $^1H$  NMR (600 MHz, Tetrachloroethane-*d*<sub>2</sub>)  $\delta$  = 7.96 (d,  $J$  = 9.3 Hz, 2H, BOD), 7.94 (d,  $J$  = 8.4 Hz, 2H, Ar), 7.71 (s, 2H, Ar), 7.61 (s, 2H, TAPP), 7.52 (d,  $J$  = 9.2 Hz, 2H,

BOD), 7.42 (d,  $J = 8.2$  Hz, 2H, Alk), 2.72 (t,  $J = 7.8$  Hz, 4H, Alk), 1.75 (p,  $J = 7.3$  Hz, 4H), 1.50 – 1.44 (m, 4H), 1.38 – 1.21 (m, 56H), 0.85 (t,  $J = 7.0$  Hz, 6H). Due to very low solubility of the compound **6** only C-H coupled signals were described according to HSQCAD spectrum.  $^{13}\text{C}$  NMR (151 MHz, Tetrachloroethane- $d_2$ )  $\delta = 130.6, 128.0, 123.1, 115.7, 112.1, 91.9, 35.7, 31.8, 31.2, 31.1, 30.5, 29.6, 29.5, 28.1, 27.2, 22.7, 22.6, 13.9$ . HRMS (EI):  $m/z$  calculated for  $\text{C}_{66}\text{H}_{86}\text{N}_6\text{O}_2$ : 994.6812 [ $\text{M}^+$ ]; found: 994.6837.

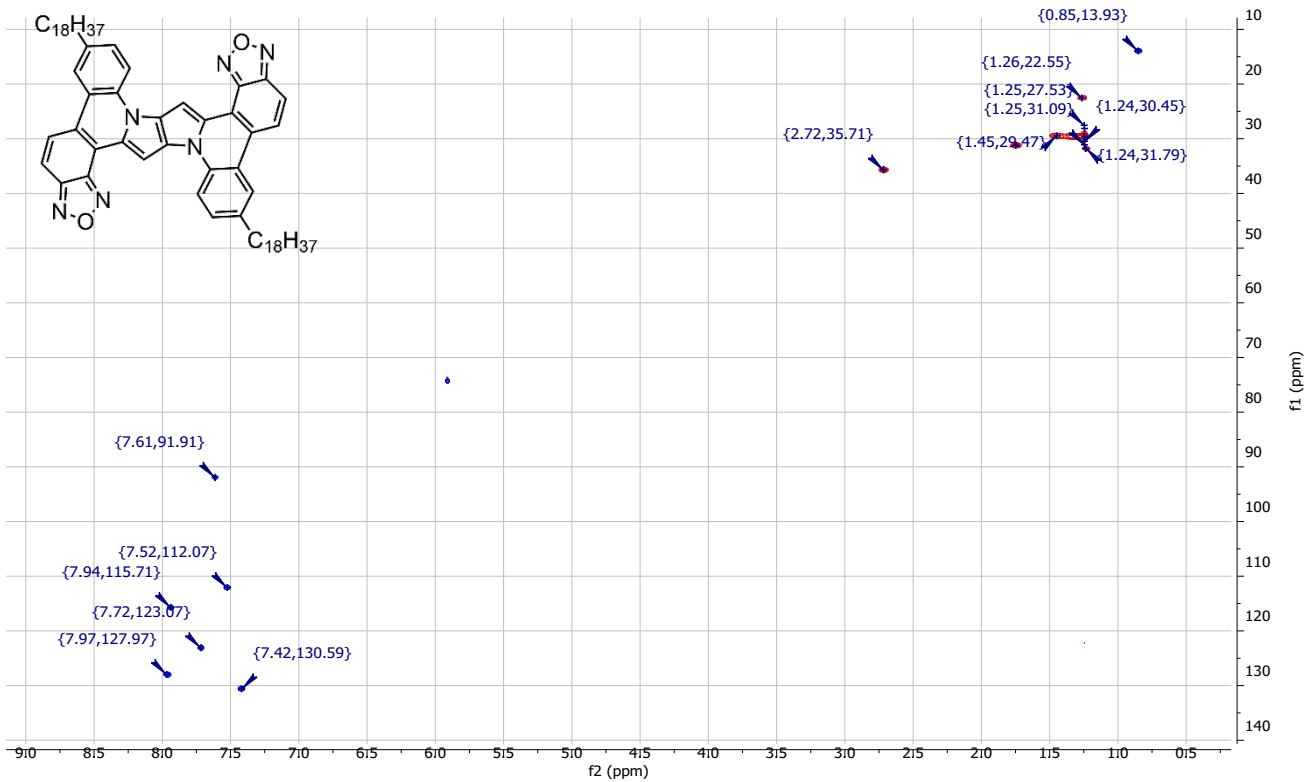
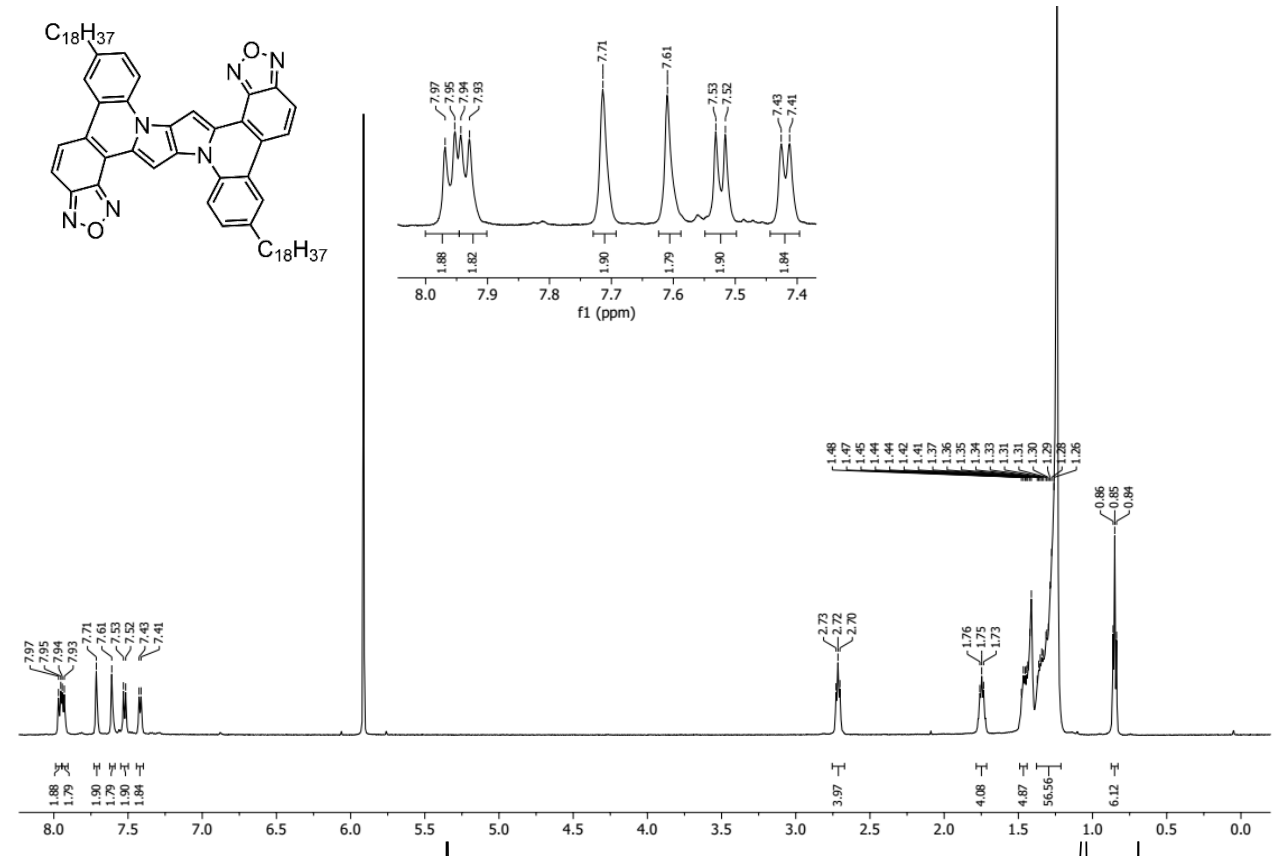
### 3. $^1\text{H}$ and $^{13}\text{C}$ NMR spectra for synthesized compounds





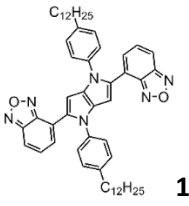






## 4. Optical properties (in solution)

Table S1

					
Solvent	$\lambda_{\text{max}}^{\text{abs}}$ [nm]	$\epsilon \cdot 10^{-4}$ [ $\text{M}^{-1} \cdot \text{cm}^{-1}$ ]	$\lambda_{\text{max}}^{\text{em}}$ [nm]	Stokes' shift [ $\text{cm}^{-1}$ ]	$\Phi^{\text{a}}$
CCl <sub>4</sub>	508	2.54	573	2 230	0.70
Cyclohexane	499	2.91	553	1 960	0.77
	511	2.91	581		
EtOH	496	2.59	666	5 150	0.01
Toluene	506	2.46	590	2 810	0.67
CH <sub>2</sub> Cl <sub>2</sub>	504	2.30	673	4 980	0.08
Dioxane	502	2.55	617	3 710	0.59
DMF	498	2.25	688	5 550	0.02
DMSO	500	2.16	708	5 880	0.02
THF	501	2.48	623	3 910	0.44

<sup>a</sup>Relative  $\Phi$  were obtained using rhodamine 6G in EtOH ( $\lambda_{\text{exc}} = 490$  nm,  $\Phi = 0.95$ ) as a reference.

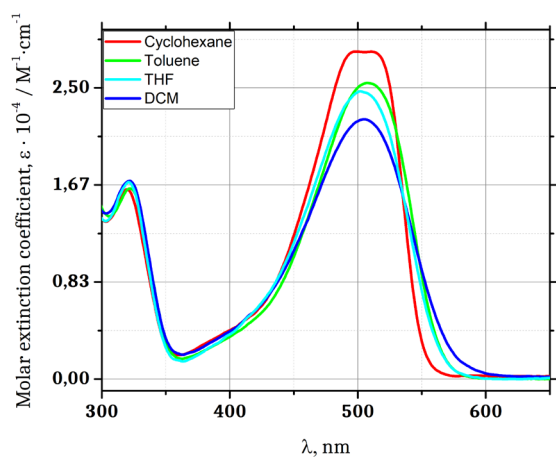


Figure S1. Absorption spectra of 1.

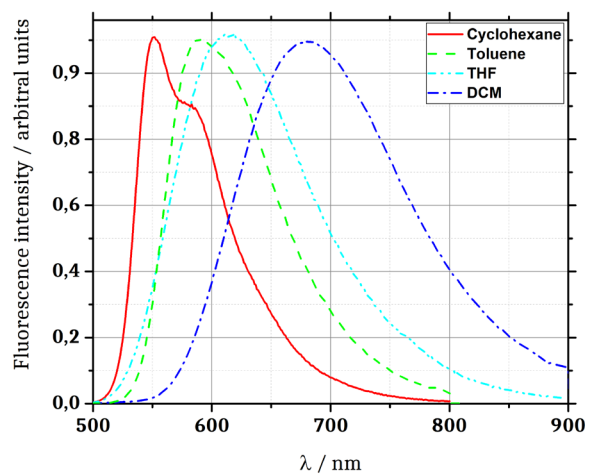


Figure S2. Emission spectra of 1.

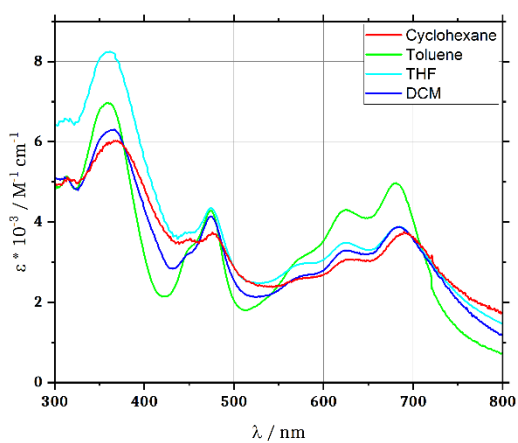


Figure S3. Absorption spectra of 6

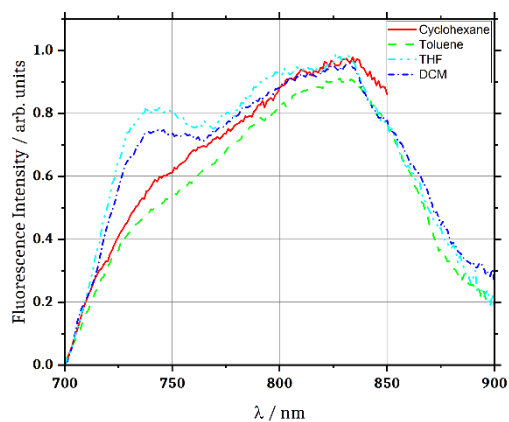


Figure S4. Emission spectra of 6

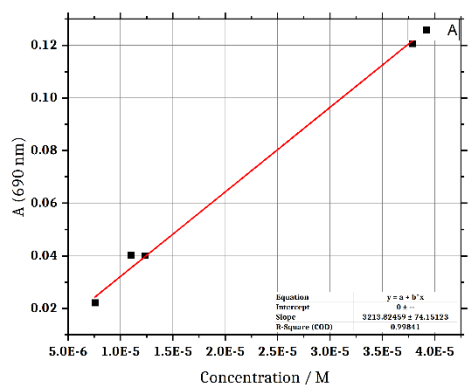


Figure S5. Absorbance on concentration for 6.

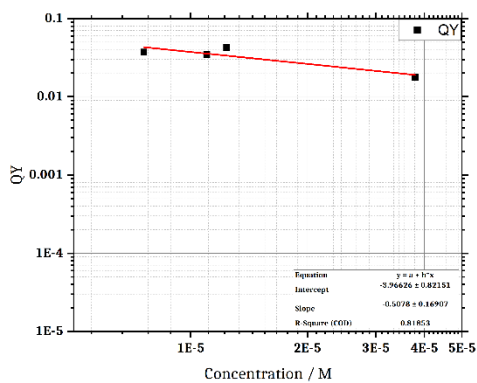


Figure S6. Quantum yield on concentration for 6.

## 5. Optical properties (in solid state)

Time-resolved photoluminescence measurements were conducted on a custom-built setup at the Chemistry Department, University of Warsaw. Laser pulses (390 nm, 2 ns pulse duration) generated by an Ekspla NT230 Nd:YAG laser were used to excite all samples. The laser light was directed to the sample through the rear port of an Olympus IX73 inverted microscope, focused by a reflective objective. To prevent UV emission and backscattering from reaching the eye and detector, a dichroic mirror and a 490 nm longpass filter were employed. Single-crystal samples were positioned on a quartz slide with a non-luminescent Olympus Type-F immersion oil, and then placed inside a nitrogen-cooled cryostat. The cryostat was equipped with a microcontroller-based heater to maintain temperatures of either 100 K or 200 K during the low-temperature measurements. The emitted light from the sample was collected through the reflective objective and directed to a spectrograph equipped with a time-gated intensified charge-coupled device (ICCD) camera (PI-MAX4, Princeton Instruments). The camera was triggered by each laser pulse, facilitating a precise control of the camera readout delay during the experiment. The LightField software (Princeton Instruments) was employed to control the camera's intensifier gating width and delay, enabling time-resolved measurements of the samples' emission. The luminescence lifetimes were determined by fitting the intensity decay data using least-squares analysis.

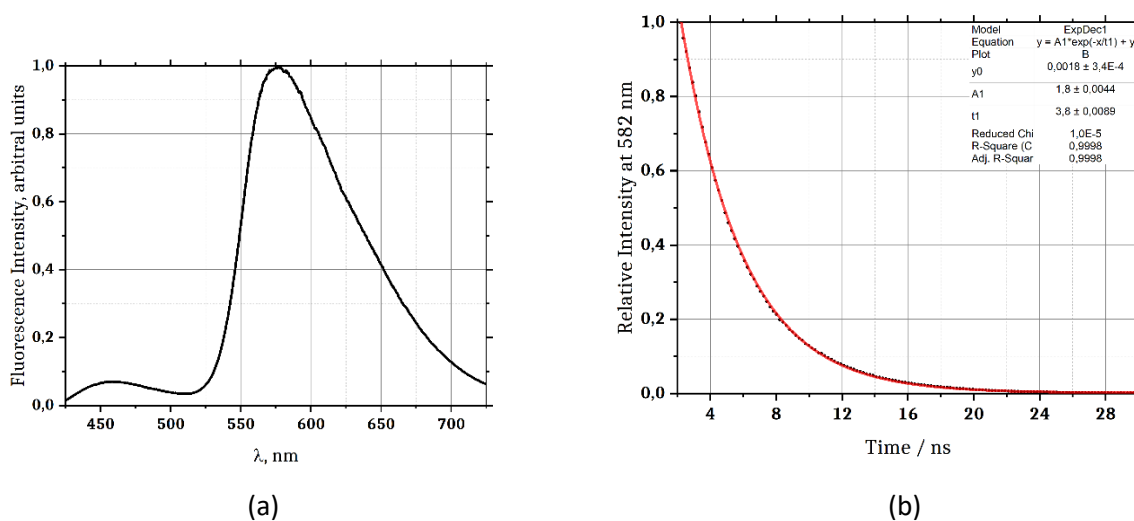


Figure S7. Solid-state emission spectrum (a) and emission decay (b) of 1 at room temperature.

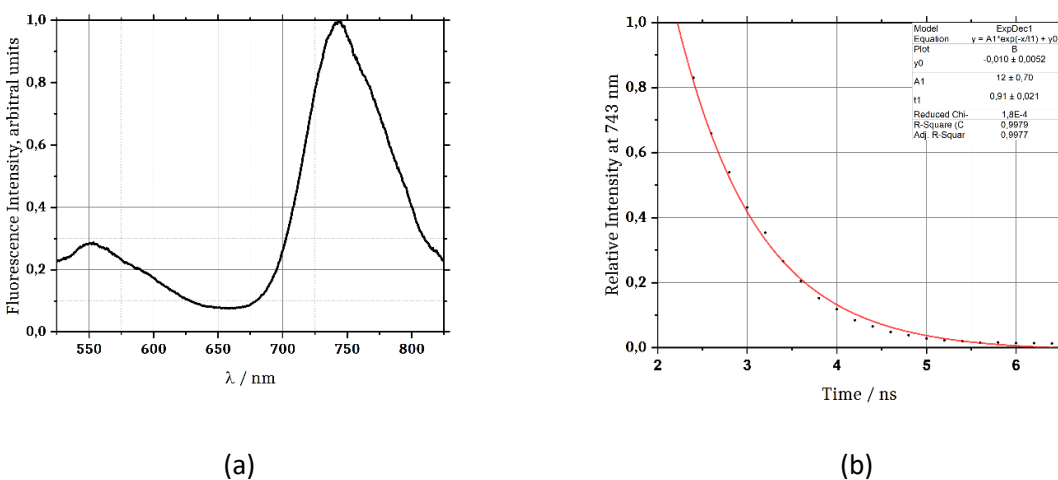
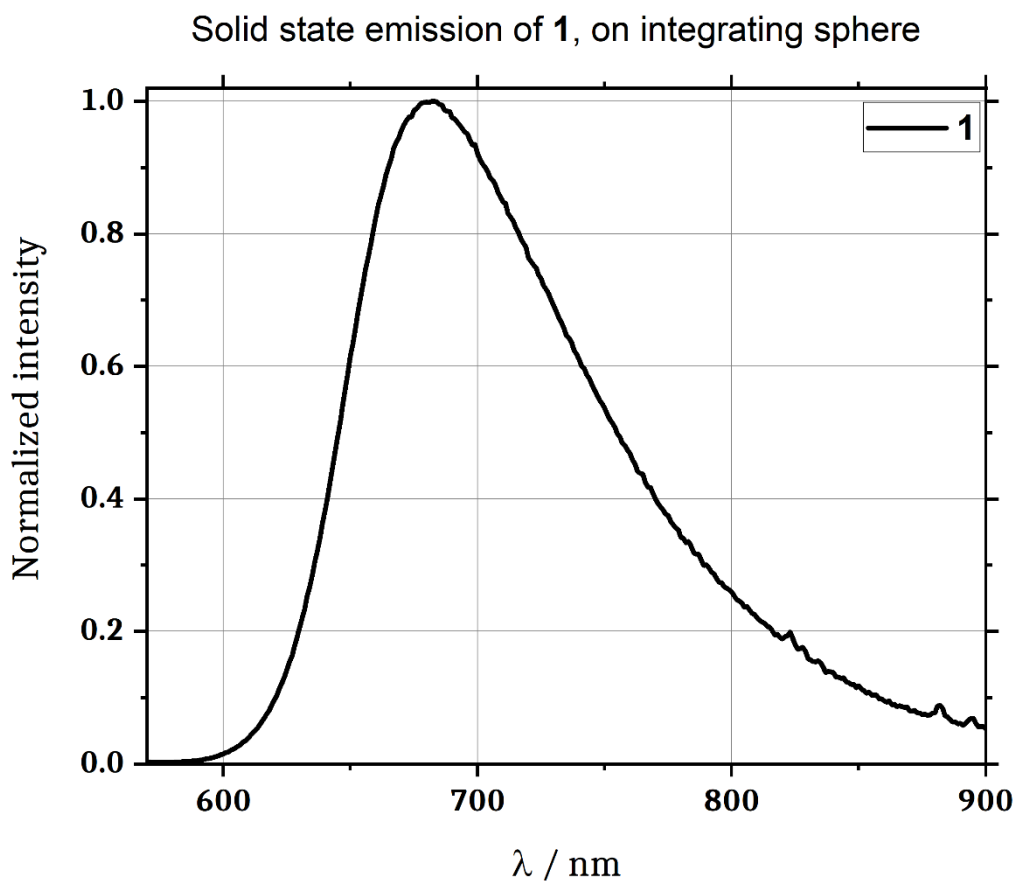


Figure S8. Solid-state emission spectrum (a) and emission decay (b) of 6 at room temperature.

Emission spectra of powder sample was measured using front-face collection mode using 0.75 nm excitation and emission bandwidths. To eliminate any background emission, the spectrum of empty cuvette was subtracted from the sample's spectra. Quantum yield was measured using an integrating sphere (Edinburgh Instruments FS5) according to the known procedure.<sup>1</sup> Sample **1** was excited at 550 nm.



**Figure S9.** Solid-state emission spectrum of **1** measured on an integrating sphere.

## 6. Crystallographic data

Single-crystal X-ray measurement was performed on a Rigaku Oxford Diffraction SuperNova instrument equipped with a copper X-ray source (Cu K $\alpha$  radiation,  $\lambda = 1.54184 \text{ \AA}$ ). During the measurement crystal was maintained at 100 K with the use of an Oxford Cryosystems nitrogen gas-flow device. Unit-cell parameter determination and raw diffraction image processing were performed with the native diffractometer CRYCALISPRO software suite. Structure was solved using an intrinsic phasing method as implemented in the SHELXT program<sup>2</sup> and refined with the OLEX2<sup>3</sup> package within the independent atom model approximation. In all cases the riding model for the hydrogen thermal motion parameters was applied ( $U_{iso}^H = x \cdot U_{eq}^H$ , where  $x = 1.2$  for X = C, and  $x = 1.5$  for X = O). The original CIF file is also available from the Supporting Information, or can be retrieved from the Cambridge Structural Database<sup>4,5</sup> (deposition number: CCDC 2288872).

<i>Data set</i>	<b>1</b>
Moiety formula	2(C <sub>27</sub> H <sub>33</sub> N <sub>3</sub> O),0.82(C H <sub>2</sub> Cl <sub>2</sub> )
Moiety formula mass, $M_r$ / a.u.	901.19
Crystal system	triclinic
Space group	$P\bar{1}$ (no. 2)
$Z$	2
$F_{000}$	965
Crystal colour & shape	Red needle
Crystal size / mm <sup>3</sup>	0.19×0.12×0.09
$T$ / K	100
$a$ / $\text{\AA}$	8.0413(5)
$b$ / $\text{\AA}$	14.3206(8)
$c$ / $\text{\AA}$	21.6156(8)
$\alpha$ / $\text{\AA}$	78.691(4)
$\beta$ / $\text{\AA}$	88.151(4)
$\gamma$ / $\text{\AA}$	87.222(5)
$V$ / $\text{\AA}^3$	2437.3(2)
$d_{\text{calc}}$ / g·cm <sup>-3</sup>	1.228
$\theta$ range	2.03°–74.87°
Absorption coefficient, $\mu$ / mm <sup>-1</sup>	1.388
No. of reflections collected / unique	38160 / 9943
$R_{\text{int}}$	6.45%
No. of reflections with $I > 3\sigma(I)$	7145
No. of parameters / restraints / constraints	589 / 0 / 5
$R[F]$ ( $I > 3\sigma(I)$ )	7.32%
$R[F]$ (all data)	9.99%
$\rho_{\text{res}}^{\text{min/max}}$ / e· $\text{\AA}^{-3}$	-0.84 / +1.27
CCDC code	2288872

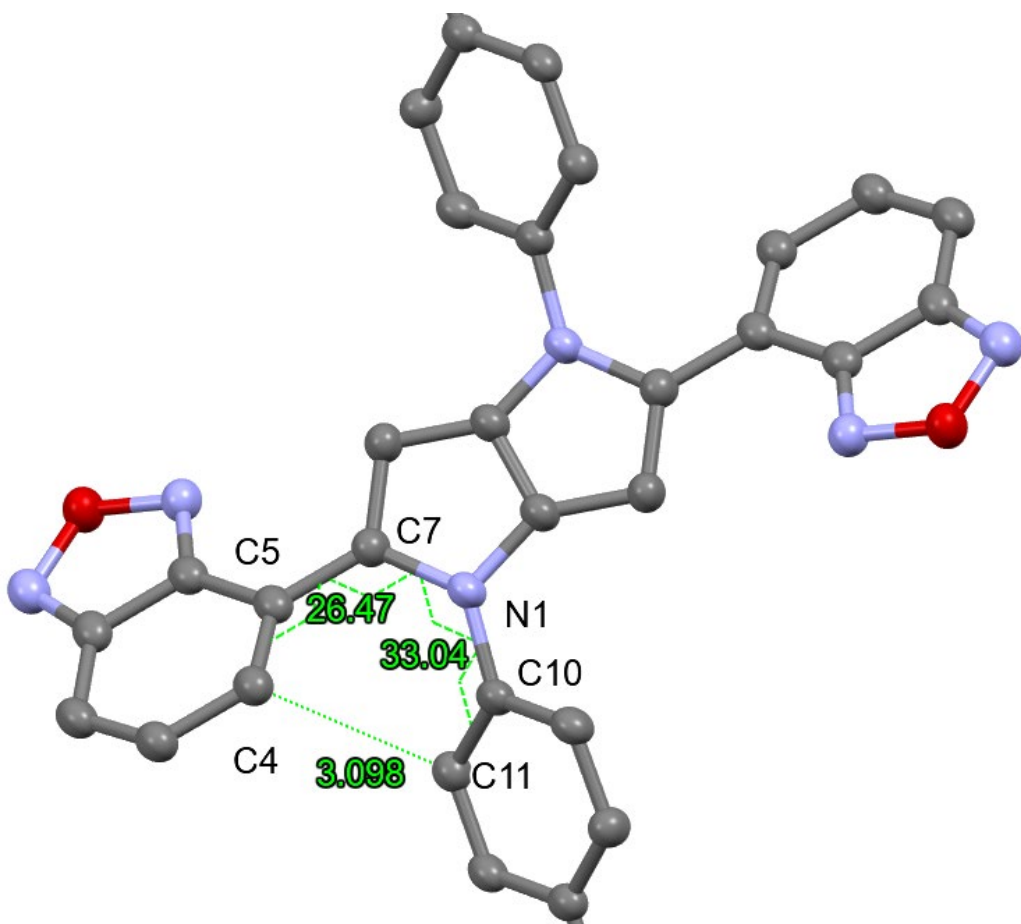


**Figure S10.** Torsion angles and the distance between C4 and C11 in **1** crystal structure. Ellipsoids correspond to 50% probability of atom location. Alkyl chains and hydrogen atoms are omitted for clarification.

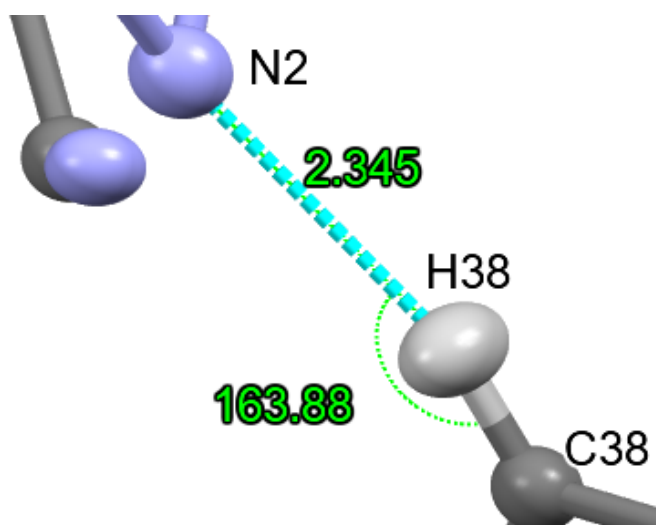


**Figure S11.** Hydrogen bond in crystal structure of **1**.

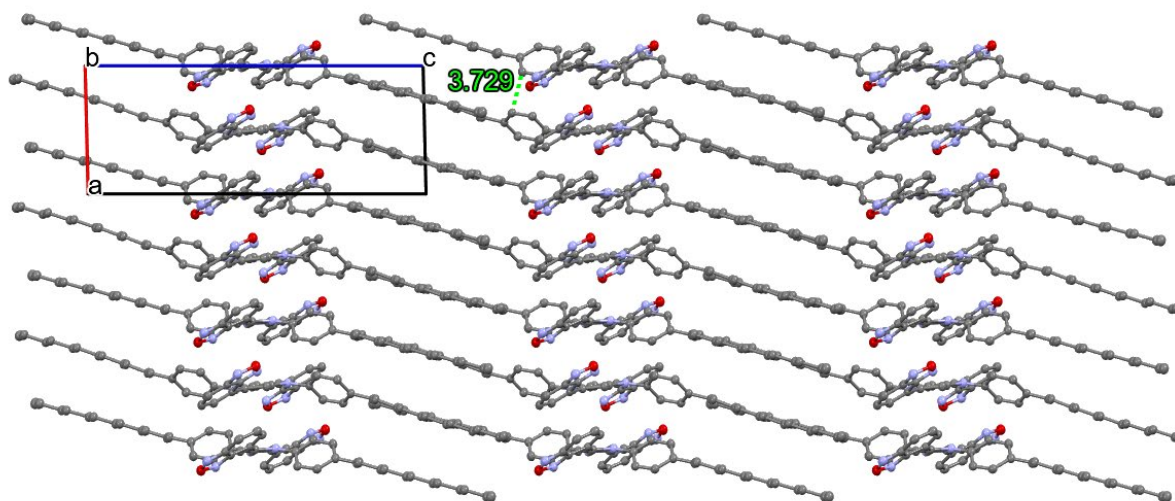


**Figure S12.** Packing 2x2 in crystal structure of **1**. Unit cell axes are shown. The distance between aromatic rings is small enough to assume that there are  $\pi$ - $\pi$  interactions in this crystal.

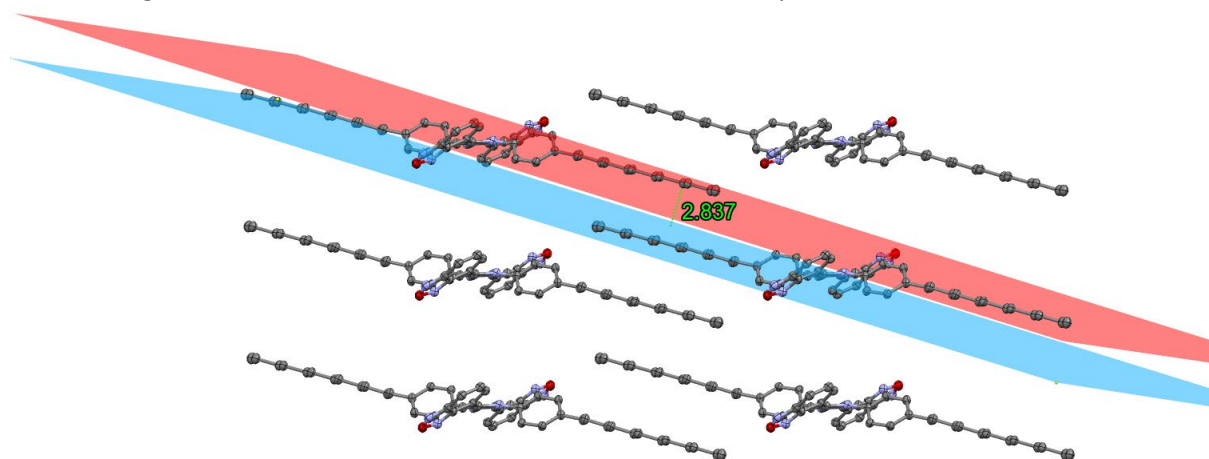


**Figure S13.** Packing in crystal structure of **1**. Distance between carbon atom from red plane and blue plane was measured.



## 7. Theoretical calculations

Ground state ( $S_0$ ) molecular electronic structures optimization of dyes **1** and **6** with ethyl chain was performed at the density functional theory (DFT) level by using B3LYP functional with the 37% of Hartree-Fock (HF) (called next as B3LYP-37)<sup>6,7</sup> and 6-31G(d,p)<sup>8,9</sup> basis set. The energy minima of the structures were confirmed by the vibrational frequency analysis which is done separately with the ground state geometries. Polarizable continuum model (PCM)<sup>10</sup> within the time-dependent density functional theory (TDDFT) level<sup>11-14</sup> and B3LYP-37/6-31G(d,p) theory were used to obtain the  $S_0 \rightarrow S_1$  vertical excitations for the dyes with various solvents with increasing solvent polarity. We employed the same TDDFT/B3LYP-37/6-31G(d, p) method to optimize the  $S_1$  state of the studied dyes in different solvents.

To estimate the spin-orbit coupling matrix elements (SOCME) and singlet-triplet intersystem crossing rates, the perturbative spin-orbit coupling (pSOC)<sup>15</sup> calculations were performed at TD-DFT approach using the ADF2023 package<sup>16</sup>. Within the scalar relativistic approximation, we used triple zeta polarized (TZP) basis<sup>17</sup> set with no frozen core, hybrid PBE0 functional<sup>18</sup> to obtain the perturbative excitation energies which include spin-orbit coupling effects. Here, SOCMEs between the respective triplet states ( $T_1, T_2$ ) and singlet ( $S_1$ ) were calculated as root mean squares that means square root of the sum of squares of spin-orbit coupling matrix elements of all sublevels of the unoccupied states<sup>19</sup>. This is given by:

$$\langle S_i | \hat{H}_{SO} | T_j \rangle = \sqrt{\sum_{m=0, \pm 1} \langle S_i | \hat{H}_{SO} | T_j^m \rangle^2} \quad (S1)$$

The spin-orbit coupling operator  $\hat{H}_{SO}$  was considered in our calculations within the zeroth-order regular approximation (ZORA)<sup>20,21</sup> in accordance with the following expression:

$$\hat{H}_{SO} = \frac{c^2}{(2c^2 - V)^2} \sigma(\nabla V \cdot p), \quad (S2)$$

where  $\sigma$  – Pauli spin matrix vector,  $\mathbf{p}$  – the linear momentum operator;  $c$  – speed of light,  $V$  – Kohn–Sham potential. The fluorescence rate constants ( $k_r$ ) were estimated according to the following relationship (expressed in atomic units)<sup>22,23</sup>:

$$k_r = \frac{1}{\tau} = \frac{2(\Delta E^2)f}{c^3}, \quad (\text{S3})$$

where  $\tau$  is radiative life of  $S_1$  state,  $\Delta E$  and  $f$  – the energy and intensity of the corresponding singlet-singlet transition calculated by TDDFT/B3LYP-37/6-31G(d, p) method.

The rate constants of intersystem crossing (ISC) between the  $S_1$  and  $T_j$  states  $E(S_1) > E(T_j)$  were estimated using the Plotnikov's simple empirical approximation:<sup>24</sup>

$$k_{S_1 \rightarrow T_j} = 10^{10} \langle S_1 | \hat{H}_{so} | T_j \rangle^2 F_{0m}, \quad (\text{S4})$$

where Franck–Condon factors ( $F_{0m}$ ) were approximated using the formula:

$$F_{0m} = \sum_n \prod_v \frac{e^{-y} y^{n_v}}{n_v!} \quad (\text{S5})$$

In Supplementary Equation (S5) Huang–Rhys factor  $y$  was assumed to be equal to 0.3 and only one average promotive mode  $\omega_v = 1400 \text{ cm}^{-1}$  was used when considering  $n_v = \Delta E(S_1 - T_j)/\omega_v$ . Such a single-mode approximation was considered efficient and accurate enough for the organic dyes and fluorophores.<sup>25–28</sup>

The  $k_{IC}$  rate constants and fluorescence quantum yield ( $\phi_f$ ) were calculated using the algorithm described in Ref.<sup>29–31</sup>. This algorithm uses computed nonadiabatic coupling matrix element (NACME) between the  $S_1$  and  $S_0$  states as the input parameter calculated by TDDFT/B3LYP-37/6-31G(d, p) method by using Gaussian 16 software.<sup>32</sup>

### Excited state ( $S_1$ ) structures and molecular orbitals

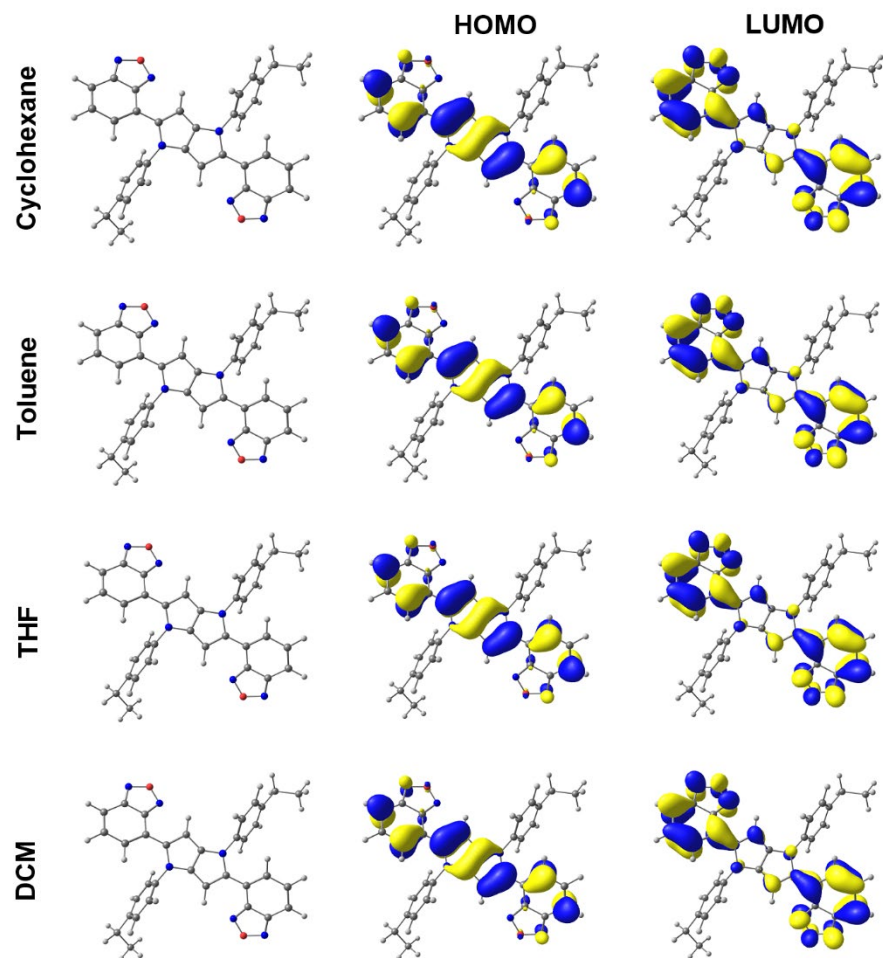


**Fig. S14.** Optimized singlet excited state ( $S_1$ ) structures and computed frontier molecular orbitals for compound **1** with -ethyl chain in different solvents.

### Excited state ( $S_1$ ) structures and molecular orbitals

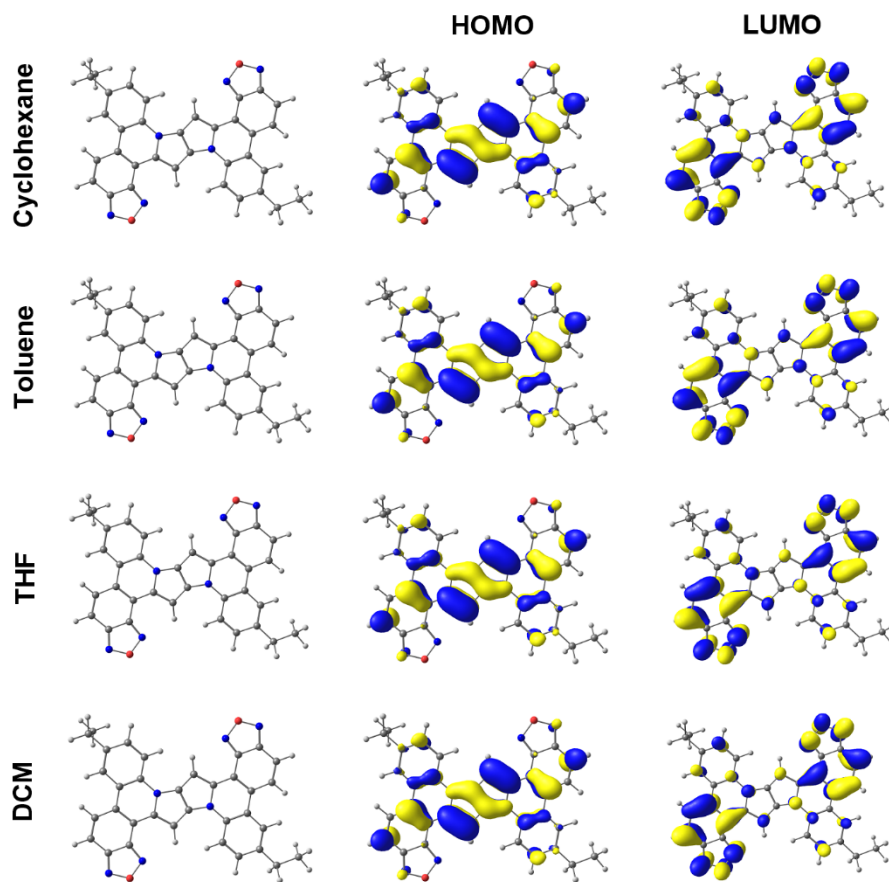


**Fig. S15.** Optimized singlet excited state ( $S_1$ ) structures and computed frontier molecular orbitals for compound **6** with -ethyl chain in different solvents.

**Table S2:** TD-DFT/PCM/B3LYP-37/6-31G (d, p) calculated optical absorption of **comp 1-C2H5**.

Solvents	Excited States	Wavelengths (nm)	Energy (eV)	Osc. Strength (f)
Cyclohexane $\epsilon= 2.016$	S1	493	2.52	0.9295
	S2	429	2.89	0.0010
	S3	373	3.32	0.0339
	S4	337	3.68	0.0004
	S5	304	4.07	0.0019
Dioxane $\epsilon= 2.21$	S1	493	2.51	0.9247
	S2	429	2.89	0.0010
	S3	374	3.32	0.0336

	S4	337	3.67	0.0004
	S5	304	4.07	0.0019
CCl4	S1	494	2.51	0.9335
$\epsilon = 2.228$	S2	430	2.88	0.0010
	S3	374	3.32	0.0341
	S4	338	3.67	0.0004
	S5	305	4.07	0.0019
Toluene	S1	495	2.50	0.9393
$\epsilon = 2.3741$	S2	431	2.88	0.0010
	S3	374	3.31	0.0343
	S4	338	3.67	0.0004
	S5	305	4.07	0.0019
THF	S1	496	2.50	0.8873
$\epsilon = 7.42$	S2	434	2.85	0.0010
	S3	377	3.29	0.0309
	S4	341	3.63	0.0003
	S5	306	4.05	0.0018
DCM	S1	496	2.50	0.8893
$\epsilon = 10.12$	S2	435	2.85	0.0010
	S3	377	3.29	0.0310
	S4	342	3.63	0.0003
	S5	306	4.05	0.0018
Acetonitrile	S1	494	2.51	0.8574
$\epsilon = 35.688$	S2	435	2.85	0.0010
	S3	377	3.29	0.0293
	S4	342	3.62	0.0003
	S5	306	4.04	0.0017

**Table S3:** TD-DFT/PCM/B3LYP-37/6-31G (d, p) calculated optical absorption of **comp 1-C8H17**.

Solvents	Excited States	Wavelengths (nm)	Energy (eV)	Osc. Strength (f)
Cyclohexane $\epsilon= 2.016$	S1	493	2.51	0.9245
	S2	429	2.89	0.0011
	S3	374	3.32	0.0356
	S4	337	3.68	0.0004
	S5	304	4.07	0.0020
Dioxane $\epsilon= 2.21$	S1	493	2.51	0.9197
	S2	430	2.89	0.0011
	S3	374	3.31	0.0352
	S4	338	3.67	0.0004
	S5	305	4.07	0.0020
CCl4 $\epsilon= 2.228$	S1	494	2.51	0.9286
	S2	430	2.88	0.0011
	S3	374	3.31	0.0357
	S4	338	3.67	0.0004
	S5	305	4.07	0.0020
Toluene $\epsilon= 2.3741$	S1	496	2.50	0.9344
	S2	431	2.88	0.0011
	S3	375	3.31	0.0359
	S4	338	3.66	0.0004
	S5	305	4.06	0.0020
THF $\epsilon= 7.42$	S1	496	2.50	0.8828
	S2	435	2.85	0.0010
	S3	377	3.29	0.0325
	S4	342	3.63	0.0004
	S5	306	4.05	0.0019
DCM	S1	497	2.50	0.8848

$\epsilon = 10.12$	S2	435	2.85	0.0010
	S3	377	3.29	0.0326
	S4	342	3.63	0.0004
	S5	306	4.05	0.0019
	Acetonitrile	S1	495	2.51
$\epsilon = 35.688$	S2	436	2.85	0.0010
	S3	377	3.29	0.0310
	S4	343	3.62	0.0003
	S5	307	4.04	0.0018

**Table S4:** TD-DFT/PCM/B3LYP-37/6-31G (d, p) calculated optical absorption of **comp 6-C2H5**.

Solvents	Excited States	Wavelengths (nm)	Energy (eV)	Osc. Strength (f)
Cyclohexane $\epsilon = 2.016$	S1	574	2.16	0.5101
	S2	487	2.55	0.0000
	S3	399	3.11	0.2805
	S4	353	3.52	0.0000
	S5	332	3.74	0.0006
Dioxane $\epsilon = 2.21$	S1	574	2.16	0.5068
	S2	488	2.54	0.0000
	S3	399	3.10	0.2800
	S4	353	3.51	0.0000
	S5	332	3.73	0.0006
CCl4 $\epsilon = 2.228$	S1	575	2.16	0.5140
	S2	488	2.54	0.0000
	S3	400	3.10	0.2853
	S4	353	3.51	0.0000
	S5	332	3.73	0.0006
Toluene $\epsilon = 2.3741$	S1	576	2.15	0.5191
	S2	489	2.54	0.0000

	S3	400	3.10	0.2902
	S4	353	3.51	0.0000
	S5	332	3.73	0.0006
THF	S1	577	2.15	0.4828
$\epsilon = 7.42$	S2	493	2.52	0.0000
	S3	402	3.09	0.2767
	S4	356	3.48	0.0000
	S5	333	3.72	0.0004
DCM	S1	577	2.15	0.4850
$\epsilon = 10.12$	S2	493	2.51	0.0000
	S3	402	3.08	0.2792
	S4	357	3.48	0.0000
	S5	333	3.72	0.0004
Acetonitrile	S1	575	2.15	0.4624
$\epsilon = 35.688$	S2	494	2.51	0.0000
	S3	402	3.08	0.2664
	S4	357	3.47	0.0000
	S5	334	3.72	0.0003

**Table S5:** TD-DFT/PCM/B3LYP-37/6-31G (d, p) calculated optical  $S1 \rightarrow S0$  emission of **comp 1-C2H5**.

Solvents	Wavelength (nm)	Energy (eV)	Osc. Strength (f)	Transition
Cyclohexane $\epsilon = 2.016$	573	2.16	1.0116	H $\rightarrow$ L (0.70134)
Toluene $\epsilon = 2.3741$	581	2.13	1.0400	H $\rightarrow$ L (0.70126)
THF $\epsilon = 7.42$	620	2.00	1.1696	H $\rightarrow$ L (-0.70075)
DCM $\epsilon = 10.12$	624	1.99	1.1817	H $\rightarrow$ L (-0.70069)



**Table S6:** TD-DFT/PCM/B3LYP-37/6-31G (d, p) calculated optical  $S_1 \rightarrow S_0$  emission of **comp 1-C8H17**.

Solvents	Wavelength (nm)	Energy (eV)	Osc. Strength (f)	Transition
Cyclohexane $\epsilon = 2.016$	573	2.16	1.0027	H $\rightarrow$ L (0.70133)
Toluene $\epsilon = 2.3741$	581	2.13	1.0314	H $\rightarrow$ L (0.70125)
THF $\epsilon = 7.42$	620	2.00	1.1648	H $\rightarrow$ L (-0.70075)
DCM $\epsilon = 10.12$	624	1.99	1.1776	H $\rightarrow$ L (-0.70070)

**Table S7:** TD-DFT/PCM/B3LYP-37/6-31G (d, p) calculated optical  $S_1 \rightarrow S_0$  emission of **comp 6-C2H5**.

Solvents	Wavelength (nm)	Energy (eV)	Osc. Strength (f)	Transition
Cyclohexane $\epsilon = 2.016$	691	1.80	0.5281	H $\rightarrow$ L (0.70137)
Toluene $\epsilon = 2.3741$	698	1.78	0.5496	H $\rightarrow$ L (0.70126)
THF $\epsilon = 7.42$	735	1.69	0.6529	H $\rightarrow$ L (0.70197)
DCM $\epsilon = 10.12$	739	1.68	0.6630	H $\rightarrow$ L (0.70198)

**Table S8.** Summary of perturbative spin-orbit coupling excitation calculations, intersystem crossing (ISC), internal conversion (IC) and radiative rate constants of **1** and **6**.

Dye	Solvent	$E_{S_1}$ / eV	$E_{T_1}$ / eV	$E_{T_2}$ / eV	SOCME $_{S_1T_1}$ / cm $^{-1}$	SOCME $_{S_1T_2}$ / cm $^{-1}$	$k_{ISC}^{S_1T_1}$ $\times 10^2$ / s $^{-1}$	$k_{ISC}^{S_1T_2}$ $\times 10^7$ / s $^{-1}$	$k_r^{(a)}$ $\times 10^8$ / s $^{-1}$	$k_{IC}^{(b)}$ $\times 10^8$ / s $^{-1}$	$\Phi_{fl}^{theor}(\Phi_{fl}^{exp})$
<b>1</b>	Cyclohexane	1.99	1.11	1.62	0.04	0.37	2.06	3.60	2.053	1.0	0.61 (0.77)
	Toluene	1.97	1.10	1.61	0.03	0.37	1.35	4.23	2.053	1.0	0.58 (0.67)
	THF	1.83	1.05	1.57	0.03	0.39	12.8	18.6	2.027	2.3	0.32 (0.44)
	DCM	1.81	1.05	1.56	0.03	0.39	13.7	19.9	2.023	2.4	0.31 (0.08)
<b>6</b>	cyclohexane	1.64	1.02	1.53	0.02	0.00	16.2	0.00	0.738	4.3	0.14 (0.01)
	toluene	1.62	1.01	1.52	0.02	0.00	17.9	0.00	0.752	4.7	0.13 (0.01)
	THF	1.53	0.98	1.48	0.01	0.00	27.8	0.00	0.805	7.0	0.10 (0.01)
	DCM	1.52	0.98	1.48	0.01	0.00	29.1	0.00	0.810	7.5	0.09 (0.01)

**Optimized geometry:**Ground state ( $S_0$ ) geometry of compound **1-C2H5** (gas phase)

6	-3.275587000	-3.213947000	0.081411000
6	-4.500600000	-3.951380000	-0.039591000
6	-3.137501000	-1.880333000	-0.459774000
6	-4.262373000	-1.403360000	-1.090754000
6	-5.484610000	-2.145611000	-1.199829000
6	-5.637983000	-3.400188000	-0.697087000
6	1.759111000	1.045507000	-0.359174000
7	1.647478000	-0.357121000	-0.361110000
6	0.299759000	-0.654255000	-0.388283000
6	-0.414357000	0.534245000	-0.432087000
6	0.489315000	1.611281000	-0.391574000
6	-0.605730000	-1.728090000	-0.314812000
6	-1.875373000	-1.162312000	-0.351922000
7	-1.762534000	0.238068000	-0.428547000
6	-2.765939000	1.225239000	-0.198551000
6	2.643416000	-1.328455000	-0.046845000
6	2.828159000	-2.418063000	-0.894773000
6	3.760865000	-3.397553000	-0.573572000
6	4.536839000	-3.307454000	0.583390000
6	4.338167000	-2.206228000	1.420547000
6	3.397308000	-1.229991000	1.121284000
6	-2.926867000	2.263325000	-1.113548000
6	-3.871714000	3.255475000	-0.878831000
6	-4.682391000	3.229802000	0.257525000
6	-4.510127000	2.177373000	1.160491000
6	-3.557698000	1.189532000	0.947732000
6	5.393434000	1.983306000	-1.149786000
6	5.531827000	3.264749000	-0.715041000
6	4.374908000	3.851083000	-0.125566000
6	3.146355000	3.120164000	-0.000586000
6	3.024373000	1.757601000	-0.468783000
6	4.168095000	1.246876000	-1.036359000
1	-4.237174000	-0.427976000	-1.544072000
1	2.241808000	-2.494144000	-1.797148000
1	3.886740000	-4.241840000	-1.235696000
1	4.913958000	-2.119319000	2.330554000
1	3.238225000	-0.399604000	1.790228000
1	-2.318333000	2.285236000	-2.004097000
1	-3.985526000	4.054519000	-1.596964000
1	-5.122012000	2.134049000	2.049817000
1	-3.424928000	0.394033000	1.663193000
1	4.156519000	0.247191000	-1.433829000
1	0.286493000	2.663138000	-0.418330000
1	-0.403235000	-2.779673000	-0.276722000
6	-5.687955000	4.328581000	0.523588000
1	-6.069361000	4.707229000	-0.424464000
1	-6.542916000	3.915188000	1.058142000

6	-5.101331000	5.495341000	1.334118000
1	-4.263566000	5.952098000	0.810784000
1	-4.739838000	5.155265000	2.302649000
6	5.581527000	-4.353107000	0.906453000
1	5.661267000	-4.462148000	1.987714000
1	5.257191000	-5.319396000	0.521419000
6	6.966115000	-4.018166000	0.329539000
1	7.333902000	-3.071414000	0.721013000
1	6.927674000	-3.935705000	-0.755187000
1	7.688308000	-4.791999000	0.583923000
1	-5.853620000	6.263592000	1.504431000
7	-4.346270000	-5.118992000	0.538856000
7	-2.413785000	-3.956312000	0.734873000
8	-3.070817000	-5.111876000	1.006476000
1	-6.554258000	-3.958989000	-0.781971000
1	-6.307229000	-1.674488000	-1.715724000
7	4.203330000	5.049631000	0.380182000
7	2.265176000	3.897555000	0.582549000
8	2.914018000	5.067605000	0.807864000
1	6.450536000	3.818999000	-0.803368000
1	6.231382000	1.484596000	-1.612336000

Ground state ( $S_0$ ) geometry of compound **1-C18H17** (gas phase)

6	0.847805000	5.315588000	0.308064000
6	1.367384000	6.653216000	0.318651000
6	1.484137000	4.261566000	-0.450052000
6	2.601894000	4.657323000	-1.146517000
6	3.117485000	5.995323000	-1.123351000
6	2.536872000	7.002001000	-0.416431000
6	-0.642637000	-1.016172000	-0.860897000
7	-1.394618000	0.149578000	-0.625689000
6	-0.504911000	1.204584000	-0.598874000
6	0.770014000	0.714316000	-0.841214000
6	0.701656000	-0.683098000	-0.985465000
6	-0.421524000	2.584915000	-0.341765000
6	0.922313000	2.918442000	-0.470227000
7	1.663859000	1.764494000	-0.783537000
6	3.075473000	1.569675000	-0.720303000
6	-2.735771000	0.261689000	-0.153229000
6	-3.622234000	1.115252000	-0.805889000
6	-4.917240000	1.271050000	-0.325129000
6	-5.361526000	0.573803000	0.799871000
6	-4.457905000	-0.279012000	1.439774000
6	-3.156177000	-0.430362000	0.981159000
6	3.734312000	0.983432000	-1.798667000
6	5.102626000	0.747877000	-1.731584000
6	5.844448000	1.100841000	-0.602636000
6	5.166525000	1.693434000	0.466177000
6	3.797031000	1.917911000	0.419977000

6	-3.047486000	-3.851309000	-1.804842000
6	-2.345767000	-4.997172000	-1.593003000
6	-1.015917000	-4.832920000	-1.109071000
6	-0.465256000	-3.531294000	-0.860413000
6	-1.231994000	-2.327403000	-1.091570000
6	-2.503901000	-2.545810000	-1.566645000
1	3.122085000	3.940337000	-1.757086000
1	-3.294343000	1.652285000	-1.682235000
1	-5.590971000	1.943669000	-0.835707000
1	-4.770112000	-0.818951000	2.321897000
1	-2.463805000	-1.072941000	1.500849000
1	3.175453000	0.721427000	-2.683503000
1	5.600440000	0.292353000	-2.575244000
1	5.715135000	1.974331000	1.353451000
1	3.286046000	2.359416000	1.260424000
1	-3.133845000	-1.702598000	-1.789399000
1	1.490313000	-1.379352000	-1.189201000
1	-1.208545000	3.279618000	-0.126677000
6	7.326937000	0.813129000	-0.521549000
1	7.763747000	0.872602000	-1.518972000
1	7.814680000	1.583998000	0.076016000
6	7.642568000	-0.567145000	0.084132000
1	7.151129000	-1.338097000	-0.511729000
1	7.201524000	-0.627826000	1.080512000
6	9.144073000	-0.858184000	0.166778000
1	9.579941000	-0.794039000	-0.833177000
1	9.630680000	-0.079672000	0.759352000
6	9.464219000	-2.229101000	0.771667000
1	8.976443000	-3.006700000	0.179413000
1	9.027678000	-2.292123000	1.771102000
6	10.965367000	-2.524202000	0.855956000
1	11.401542000	-2.462092000	-0.143984000
1	11.453051000	-1.745440000	1.447308000
6	11.285698000	-3.894053000	1.462573000
1	10.798276000	-4.673377000	0.871765000
1	10.849961000	-3.956637000	2.462689000
6	12.786391000	-4.190786000	1.547561000
1	13.222314000	-4.129853000	0.548269000
1	13.274092000	-3.412606000	2.138259000
6	13.098626000	-5.559922000	2.155003000
1	12.654501000	-6.362415000	1.566716000
1	12.706504000	-5.639862000	3.168506000
1	14.171749000	-5.737964000	2.200479000
6	-6.784260000	0.712960000	1.293329000
1	-6.804110000	0.603551000	2.378046000
1	-7.146458000	1.718489000	1.077753000
6	-7.746762000	-0.313195000	0.667400000
1	-7.381780000	-1.319726000	0.879943000
1	-7.725109000	-0.205417000	-0.418645000
6	-9.186636000	-0.171045000	1.170082000

1	-9.200801000	-0.275631000	2.257538000
1	-9.544210000	0.839512000	0.958805000
6	-10.150476000	-1.188713000	0.551145000
1	-9.792088000	-2.198941000	0.762548000
1	-10.135473000	-1.083779000	-0.536283000
6	-11.591466000	-1.048288000	1.052675000
1	-11.605992000	-1.153024000	2.140159000
1	-11.949277000	-0.037722000	0.841612000
6	-12.556227000	-2.065141000	0.434386000
1	-12.199171000	-3.076165000	0.645316000
1	-12.542462000	-1.960832000	-0.653322000
6	-13.997328000	-1.925289000	0.935470000
1	-14.011975000	-2.030342000	2.022190000
1	-14.355064000	-0.915493000	0.724374000
6	-14.955336000	-2.943601000	0.314015000
1	-14.644864000	-3.963955000	0.537325000
1	-14.990679000	-2.840674000	-0.770214000
1	-15.968510000	-2.816126000	0.691494000
7	0.759371000	-3.683229000	-0.415401000
7	-0.110473000	-5.735146000	-0.812678000
8	0.967735000	-5.023695000	-0.391998000
7	0.601829000	7.394615000	1.084114000
7	-0.217517000	5.284331000	1.072837000
8	-0.361359000	6.550781000	1.537791000
1	2.921740000	8.007329000	-0.401785000
1	4.002894000	6.196322000	-1.706847000
1	-4.058682000	-3.907529000	-2.177874000
1	-2.752451000	-5.977185000	-1.775221000

Ground state ( $S_0$ ) geometry of compound **6-C2H5** (gas phase)

6	-0.310488000	-0.643587000	-0.030303000
6	0.373184000	0.579434000	-0.069610000
6	-0.556372000	1.637762000	-0.075733000
6	-1.802997000	1.032337000	-0.040543000
7	-1.660971000	-0.368446000	-0.012775000
6	0.619304000	-1.701815000	-0.020545000
6	1.865803000	-1.096586000	-0.054766000
7	1.723780000	0.304290000	-0.085806000
6	-3.119062000	1.580861000	-0.028635000
6	-4.245474000	0.763404000	0.009426000
6	-4.060778000	-0.688967000	0.037020000
6	-2.756839000	-1.230644000	0.024934000
6	3.181737000	-1.645891000	-0.060116000
6	4.308513000	-0.829416000	-0.095327000
6	4.124612000	0.623115000	-0.129815000
6	2.819253000	1.167376000	-0.126283000

6	-5.141288000	-1.593642000	0.075682000
6	-4.975607000	-2.966880000	0.101571000
6	-3.663891000	-3.463968000	0.088040000
6	-2.576142000	-2.618472000	0.050541000
6	5.201143000	1.528083000	-0.172336000
6	5.033723000	2.902763000	-0.209706000
6	3.725566000	3.402089000	-0.209322000
6	2.637519000	2.553361000	-0.168628000
6	-3.350692000	3.002253000	-0.054871000
6	-4.673227000	3.545121000	-0.042407000
6	-5.810809000	2.685883000	-0.003283000
6	-5.569825000	1.351766000	0.020908000
6	3.413160000	-3.067276000	-0.028414000
6	4.735794000	-3.610183000	-0.032265000
6	5.873770000	-2.751296000	-0.067612000
6	5.632863000	-1.417235000	-0.097251000
7	2.560096000	-4.061316000	0.006847000
8	3.323478000	-5.186040000	0.024336000
7	4.656551000	-4.916934000	0.000558000
7	-2.497834000	3.996448000	-0.091617000
8	-3.261420000	5.121257000	-0.101814000
7	-4.594311000	4.851935000	-0.071840000
1	-0.408310000	2.696610000	-0.099542000
1	0.471220000	-2.760578000	0.007723000
1	6.208976000	1.148956000	-0.179982000
1	3.557741000	4.468340000	-0.246426000
1	1.646242000	2.965257000	-0.175935000
1	6.482117000	-0.758079000	-0.123608000
1	6.871499000	-3.155781000	-0.069993000
1	-1.585617000	-3.032213000	0.040789000
1	-3.496850000	-4.531092000	0.107221000
1	-6.141828000	-1.203157000	0.085615000
1	-6.419398000	0.693236000	0.050496000
1	-6.808560000	3.090239000	0.006174000
6	6.222974000	3.838075000	-0.218072000
1	7.083055000	3.326582000	-0.649188000
1	6.010531000	4.685301000	-0.870287000
6	6.591563000	4.358556000	1.180127000
1	6.846095000	3.537063000	1.847248000
1	5.761437000	4.902150000	1.627401000
1	7.446083000	5.031107000	1.129256000
6	-6.134138000	-3.947904000	0.143206000
1	-6.045039000	-4.618241000	-0.713813000
1	-6.012044000	-4.583434000	1.022374000
6	-7.539689000	-3.348027000	0.157887000
1	-7.732322000	-2.751599000	-0.732388000
1	-7.698528000	-2.715642000	1.029837000
1	-8.283124000	-4.141289000	0.188284000

## 8. References

1. de Mello, J. C., Wittmann, H. F. & Friend, R. H. An improved experimental determination of external photoluminescence quantum efficiency. *Adv. Mater.* **9**, 230–232 (1997).
2. Sheldrick, G. M. Crystal structure refinement with SHELXL. *Acta Crystallogr. Sect. C* **71**, 3–8 (2015).
3. Dolomanov, O. V, Bourhis, L. J., Gildea, R. J., Howard, J. A. K. & Puschmann, H. OLEX2: a complete structure solution, refinement and analysis program. *J. Appl. Crystallogr.* **42**, 339–341 (2009).
4. Allen, F. H. The Cambridge Structural Database: a quarter of a million crystal structures and rising. *Acta Crystallogr. Sect. B* **58**, 380–388 (2002).
5. Groom, C. R., Bruno, I. J., Lightfoot, M. P. & Ward, S. C. The Cambridge Structural Database. *Acta Crystallogr. Sect. B* **72**, 171–179 (2016).
6. Becke, A. D. Density-functional thermochemistry. III. The role of exact exchange. *J. Chem. Phys.* **98**, 5648–5652 (1993).
7. Lee, C., Yang, W. & Parr, R. G. Development of the Colle-Salvetti correlation-energy formula into a functional of the electron density. *Phys. Rev. B* **37**, 785–789 (1988).
8. Ditchfield, R., Hehre, W. J. & Pople, J. A. Self-Consistent Molecular-Orbital Methods. IX. An Extended Gaussian-Type Basis for Molecular-Orbital Studies of Organic Molecules. *J. Chem. Phys.* **54**, 724–728 (2003).
9. Frisch, M. J., Pople, J. A. & Binkley, J. S. Self-consistent molecular orbital methods 25. Supplementary functions for Gaussian basis sets. *J. Chem. Phys.* **80**, 3265–3269 (1984).
10. Tomasi, J., Mennucci, B. & Cammi, R. Quantum Mechanical Continuum Solvation Models. *Chem. Rev.* **105**, 2999–3094 (2005).
11. Bauernschmitt, R. & Ahlrichs, R. Treatment of electronic excitations within the adiabatic approximation of time dependent density functional theory. *Chem. Phys. Lett.* **256**, 454–464 (1996).
12. Casida, M. E., Jamorski, C., Casida, K. C. & Salahub, D. R. Molecular excitation energies to high-lying bound states from time-dependent density-functional response theory: Characterization and correction of the time-dependent local density approximation ionization threshold. *J. Chem. Phys.* **108**, 4439–4449 (1998).
13. Stratmann, R. E., Scuseria, G. E. & Frisch, M. J. An efficient implementation of time-dependent density-functional theory for the calculation of excitation energies of large molecules. *J. Chem. Phys.* **109**, 8218–8224 (1998).
14. Scalmani, G. *et al.* Geometries and properties of excited states in the gas phase and in solution: Theory and application of a time-dependent density functional theory polarizable continuum model. *J. Chem. Phys.* **124**, 94107 (2006).
15. Wang, F. & Ziegler, T. A simplified relativistic time-dependent density-functional theory formalism for the calculations of excitation energies including spin-orbit coupling effect. *J. Chem. Phys.* **123**, 154102 (2005).
16. te Velde, G. *et al.* Chemistry with ADF. *J. Comput. Chem.* **22**, 931–967 (2001).
17. Van Lenthe, E. & Baerends, E. J. Optimized Slater-type basis sets for the elements 1–118. *J. Comput. Chem.* **24**, 1142–1156 (2003).
18. Adamo, C. & Barone, V. Toward reliable density functional methods without adjustable



- parameters: The PBE0 model. *J. Chem. Phys.* **110**, 6158–6170 (1999).
19. Samanta, P. K., Kim, D., Coropceanu, V. & Brédas, J.-L. Up-Conversion Intersystem Crossing Rates in Organic Emitters for Thermally Activated Delayed Fluorescence: Impact of the Nature of Singlet vs Triplet Excited States. *J. Am. Chem. Soc.* **139**, 4042–4051 (2017).
  20. van Lenthe, E., Snijders, J. G. & Baerends, E. J. The zero-order regular approximation for relativistic effects: The effect of spin–orbit coupling in closed shell molecules. *J. Chem. Phys.* **105**, 6505–6516 (1996).
  21. van Lenthe, E., van Leeuwen, R., Baerends, E. J. & Snijders, J. G. Relativistic regular two-component Hamiltonians. *Int. J. Quantum Chem.* **57**, 281–293 (1996).
  22. Mori, K., Goumans, T. P. M., van Lenthe, E. & Wang, F. Predicting phosphorescent lifetimes and zero-field splitting of organometallic complexes with time-dependent density functional theory including spin–orbit coupling. *Phys. Chem. Chem. Phys.* **16**, 14523–14530 (2014).
  23. Baryshnikov, G., Minaev, B. & Ågren, H. Theory and Calculation of the Phosphorescence Phenomenon. *Chem. Rev.* **117**, 6500–6537 (2017).
  24. Plotnikov, V. G. Regularities of the processes of radiationless conversion in polyatomic molecules. *Int. J. Quantum Chem.* **16**, 527–541 (1979).
  25. Baryshnikov, G. V *et al.* Benzoannelated aza-, oxa- and azaoxa[8]circulenes as promising blue organic emitters. *Phys. Chem. Chem. Phys.* **18**, 28040–28051 (2016).
  26. Valiev, R. R., Cherepanov, V. N., Artyukhov, V. Y. & Sundholm, D. Computational studies of photophysical properties of porphin, tetraphenylporphyrin and tetrabenzoporphyrin. *Phys. Chem. Chem. Phys.* **14**, 11508–11517 (2012).
  27. Artyukhov, V. Y. *et al.* A combined theoretical and experimental study on molecular photonics. *Russ. Phys. J.* **51**, 1097–1111 (2008).
  28. Valiev, R. R. *et al.* The computational and experimental investigations of photophysical and spectroscopic properties of BF<sub>2</sub> dipyrromethene complexes. *Spectrochim. Acta Part A Mol. Biomol. Spectrosc.* **117**, 323–329 (2014).
  29. Valiev, R. R. *et al.* Internal conversion rate constant calculations considering Duschinsky, anharmonic and Herzberg–Teller effects. *Phys. Chem. Chem. Phys.* **25**, 6406–6415 (2023).
  30. Valiev, R. R. *et al.* Fast estimation of the internal conversion rate constant in photophysical applications. *Phys. Chem. Chem. Phys.* **23**, 6344–6348 (2021).
  31. Valiev, R. R. *et al.* First-principles calculations of anharmonic and deuteration effects on the photophysical properties of polyacenes and porphyrinoids. *Phys. Chem. Chem. Phys.* **22**, 22314–22323 (2020).
  32. Frisch, M. J. *et al.* G16\_C01. Gaussian 16, Revision C.01, Gaussian, Inc., Wallin (2016).